

STUDY OF INTERFACIAL ADHESION OF PAVEMENT SEALANTS BASED ON MOLECULAR DYNAMICS

ŠTUDIJA MEDPLOSKOVNE ADHEZIJE TESNILA ZA PLOČNIKE S POMOČJO MOLEKULARNE DINAMIKE

Xiaofeng Huang¹, Junhui Luo¹, Cheng Xie¹, Dadi Cheng², Pengfei Tang^{3,*},
Gang Li³, Jie Chen¹

¹Guangxi Beitou Transportation Maintenance Technology Group Co., Ltd., Nanning, China

²Guangxi Weihang Road Engineering Co., Ltd., Nanning, China

³Guangxi Communications Design Group Co., Ltd., Nanning, China

Prejem rokopisa – received: 2022-11-04; sprejem za objavo – accepted for publication: 2022-12-09

doi:10.17222/mit.2022.679

To study the performance of bitumen mixture pavement sealants from their micro-mechanisms, the physical properties of base bitumen, SBS-modified bitumen and epoxy resin sealant as well as the adhesive properties of sealant-aggregate interfaces were studied using a molecular dynamics simulation. The adhesion of a sealant-pavement crack wall was studied using a contact angle test based on the surface energy theory. The results show that the epoxy resin sealant has excellent adhesion properties. Its physical properties and interfacial adhesion work are more significant than those of base bitumen and SBS-modified bitumen. An increase in the SBS can improve base bitumen's mechanical properties and interfacial interaction. The interaction between three kinds of crack sealants and aggregate is identified as mainly the physical adsorption behavior. The van der Waals force plays a significant role in the adhesion behavior of bitumen crack sealant-aggregate interface. In contrast, the electrostatic force and van der Waals forces significantly affect the epoxy resin binder-aggregate interface. The adhesion work of 90# base bitumen, SBS-modified bitumen and epoxy resin binder for the asphalt pavement crack wall is (37.76, 44.86 and 77.63) mJ/m², respectively.

Keywords: bitumen, molecular dynamics, sealant, epoxy resin

Predstavljena je raziskava lastnosti bitumenske mešanice za tesnenje pločnikov od mikromehanizma, fizikalnih lastnosti bitumenske osnove, bitumna modificiranega s SBS (Stiren-Butadien-Stiren), tesnila na osnovi epoksidne smole, kot tudi adhezivnih lastnosti na meji med tesnilom in agregatom (pesek, zdrobljeno kamenje itd.), ki so jih raziskovali s pomočjo simulacij molekularne dinamike. Adhezijo na steni razpoke pločnika in tesnila so raziskovali s testom kontaktnega kota, ki temelji na teoriji za površinsko energijo. Rezultati so pokazali, da ima epoksidno tesnilo odlične adhezijske lastnosti. Medploskovno adhezijsko delo in njegove fizikalne lastnosti so bolj pomembne kot osnovni bitumenski model ali uporaba bitumna modificiranega s SBS. Povečanje vsebnosti SBS lahko izboljša mehanske lastnosti bitumenske osnove in medploskovno interakcijo. Interakcija med tremi uporabljenimi vrstami tesnila razpok in agregatom je v glavnem fizikalna adsorpcija. Van der Waalove sile igrajo pomembno vlogo pri adhezijskem obnašanju na meji med bitumenskim tesnilom za razpoke in agregatom. V nasprotju, elektrostatične sile in Van der Waalove sile pomembno vplivajo na mejo med vezivom na osnovi epoksidne smole in agregatom. Adhezijsko delo med bitumensko osnovo 90 # in razpoko stene asfaltne pločnika je 37,76 mJ/m², pri uporabi bitumna modificiranega s SBS je 44,86 mJ/m² in uporabi veziva na osnovi epoksidne smole je 77,63 mJ/m².

Ključne besede: bitumen, molekularna dinamika, tesnilo, epoksidna smola

1 INTRODUCTION

Bitumen is a complex mixture containing a variety of organic molecules with different molecular weights, polarities and functional groups. Asphalt pavement is prone to cracks under the combined effects of climate, traffic load and environment.¹ If these cracks are not repaired, they affect driving comfort and service life.² Studies have shown that crack-filling treatment can effectively slow down road damage and extend the service life of a pavement.^{3,4}

Research on asphalt-pavement crack-grouting materials is actively carried out worldwide. Bitumen-grouting materials were mainly used in the early stage. At present, the commonly used asphalt-pavement sealants mainly in-

clude hot bitumen⁵, emulsified bitumen^{6,7} and some chemical sealants.^{8,9} The bitumen-grouting material is the most commonly used because of its relatively simple preparation and use. However, the permeability of hot bitumen joint filler in cracks is greatly influenced by temperature. Bonding failure often occurs at high temperatures, and brittle fractures can quickly occur at low temperatures.¹⁰ The viscosity of emulsified bitumen is lower than that of hot bitumen. It has high fluidity, low tensile strength and low-temperature elongation, but it easily causes bonding and cohesive failure, which needs to be repaired repeatedly.^{6,11} Due to the limitations of bitumen materials, chemical grouting materials have been used for crack repair. Adjusting the proportion of each component of the chemical grouting material can optimize the material performance, control the curing time of the slurry, and make up for the shortcomings of the bi-

*Corresponding author's e-mail:
jebbblues@163.com (Pengfei Tang)

tumen-based grouting material, such as poor fluidity, insufficient high-temperature performance and inconvenient construction. The topic has gradually become a research hotspot. Epoxy resin has excellent adhesive strength,^{12,13} and the chemical cross-linking reaction product between the curing agent and epoxy resin has good cohesiveness, which can significantly improve the high-temperature strength and deformation resistance of the adhesive.¹⁴ In addition, the epoxy resin polymer cured by a curing agent has excellent mechanical properties, so it is an ideal chemical grouting material.

In road-pavement bitumen materials, molecular dynamics simulation can effectively and intuitively characterize the molecular model and nanostructure of bitumen binder and quantitatively evaluate its physical and mechanical properties.^{15–18} It provides a practical and considerable test and evaluation method for profoundly understanding and revealing the performance evolution and attenuation mechanism of bitumen materials at the molecular scale. This indicates that molecular dynamics simulations can be used to understand the interaction at the crack-filling interface and provide valuable insights, linking the crack filling to its macroscopic performance.

In this research, the physical properties and interfacial adhesion properties of base bitumen, SBS-modified bitumen and epoxy resin binder were studied using molecular dynamics simulation. Firstly, molecular models of three kinds of sealants were constructed to calculate the modified bitumen's physical and mechanical properties. A model of sealant and α -quartz/calcite interface was also constructed to calculate the interaction energy of different sealant-aggregate interfaces. Finally, based on the surface energy theory, the surface energy of the crack sealant-crack wall interface was calculated using

the contact angle. The molecular simulation results were verified with a macroscopic test.

2 MODEL BUILDING

2.1 Bitumen model

This research used the Materials Studio (MS) software to establish the molecular models of base bitumen, SBS-modified bitumen and epoxy resin sealant, while the force field was COMPASS II. The base bitumen was selected from the four-component 12-molecule bitumen model of AAA-1 bitumen proposed by Li and Greenfield¹⁹ in 2014. The basic information about various compounds is shown in **Table 1**. The linear SBS structure (SBS-L) constructed by Dan et al.²⁰ through continuous polymerization of styrene and butadiene was used to blend the SBS molecules with the molecules of the base bitumen model in a box to obtain the original SBS-modified bitumen model, as shown in **Figure 1b**. The molecular formula of SBS is $C_{108}H_{116}$, and the relative atomic mass is 1414.1. In the simulation, SBS molecules did not break the chemical bonds to form a new structure, so SBS and bitumen were physically blended. An epoxy resin sealant was prepared using bisphenol A epoxy resin, the thiol curing agent and polypropylene glycol diglycidyl ether diluent. The specific parameters are shown in **Table 2**.

Firstly, monomer structure models of the bitumen 12 component, epoxy resin 3 component and SBS molecular chain were established, and each molecule's energy minimization and geometric optimization were carried out to make the small molecule system stable. Then, the Amorphous Cell module in MS was used to construct the molecular box. Each molecule was integrated into the

Table 1: Details of the AAA-1 bitumen model system

Components	Molecular label	Molecular formula	Number of atoms	Molar mass (g/mol)	Number in the model system	Mass ratio (%)
Asphaltene	Pyrrole	$C_{66}H_{81}N$	148	888.4	2	5.45
	Phenol	$C_{42}H_{54}O$	97	574.9	3	5.29
	Thiophene	$C_{51}H_{62}S$	114	707.1	3	6.51
Resin	Quinolinhopane	$C_{40}H_{59}N$	100	553.9	4	6.80
	Benzobisbenzothiophene	$C_{184}H_{10}S_2$	30	290.4	15	13.36
	Thioisorenieratane	$C_{40}H_{60}S$	101	573.0	4	7.03
	Pyridinhopane	$C_{36}H_{57}N$	94	503.9	4	6.18
	Trimethylbenzene-oxane	$C_{29}H_{50}O$	80	414.7	5	6.36
Saturate	Squalane	$C_{30}H_{62}$	92	422.8	4	5.19
	Hopane	$C_{35}H_{62}$	97	482.9	4	5.93
Aromatic	PHPN	$C_{35}H_{44}$	79	464.7	11	15.68
	DOCHN	$C_{30}H_{46}$	76	406.7	13	16.22

Table 2: Details of the epoxy resin model system

Components	Molecular label	Molecular formula	Number of atoms	Molar mass (g/mol)	Number in the model system	Mass ratio (%)
Epoxy resin	DGEBA	$C_{21}H_{24}O_4$	49	232.3	20	35.6
Curing agent	3-mercaptopropionate	$C_{15}H_{26}O_6S_3$	50	398.6	10	30.5
Diluent	PPGDGE	$C_{21}H_{46}O_9$	76	442.6	10	33.9

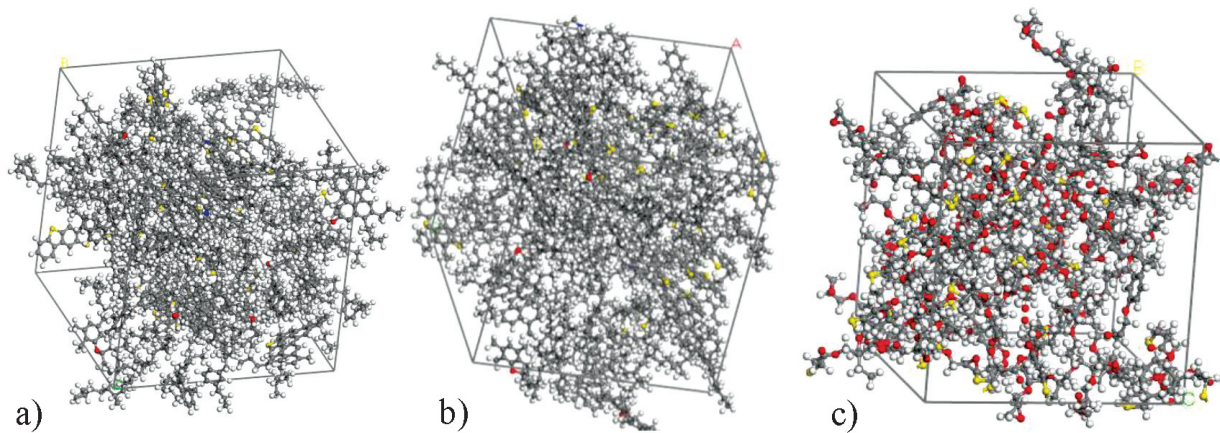


Figure 1: Three molecular models of sealants: a) base bitumen, b) SBS-modified bitumen, c) epoxy resin binder

Table 3: Detailed information about silica and calcite crystals

Mineral types	Chemical formula	Lattice parameters	Space group
Silica	α - SiO ₂	$a = b = 0.491$ nm, $c = 0.5402$ nm $\alpha = \beta = 90^\circ$, $\gamma = 120^\circ$	P3221
Calcite	CaCO ₃	$a = b = 0.499$ nm, $c = 1.7061$ nm $\alpha = \beta = 90^\circ$, $\gamma = 120^\circ$	R-3C

box in proportion to build the initial model of base bitumen, SBS-modified bitumen and epoxy resin binder. The initial density was set to 0.7 g/cm³, and the truncation radius was 1.55 nm. Each molecule was constructed for 10 frames, and the frame with the minor energy in 10 frames was selected for the geometric optimization and annealing relaxation. The NVT simulation of 200 ps was carried out in the initial base bitumen and SBS-modified bitumen model. A Nose-Hoover thermostat was used to control the constant temperature to make the system initially stable. The NPT simulation of 300 ps was carried out, and the system's density was stabilized using Andersen's constant pressure controller to control the constant pressure. Finally, a 100 ps NVT simulation was carried out to stabilize the system further. Finally, the molecular models of base bitumen and SBS-modified bitumen were obtained, as shown in **Figures 1a** and **1b**. The carbon atom is gray, hydrogen atom is white, nitrogen atom is blue, sulfur atom is yellow, and oxygen atom is red. The constructed epoxy resin sealant was cross-linked with Perl script, and the above bitumen sealant was the same. Finally, the molecular model of the epoxy resin sealant was obtained, as shown in **Figure 1c**.

2.2 Aggregate molecular model

The aggregate used in bitumen concrete is mainly composed of silica, calcite, mica and feldspar. Using X-ray diffraction, the researchers found that silica and calcite are the main chemical components of acidic and alkaline aggregates.²¹ Therefore, in this study, fine silica and calcite crystals represent acidic and alkaline aggregates. **Table 3** lists detailed information on these two minerals.

The first step in the aggregate construction is to cross-sectionalize aggregates to study the surfaces that are typically exposed. In this paper, the Miller symbol system is used to describe the anisotropic surface of minerals. For α -quartz crystals, the low Miller index surface {001} is often used as the stable surface²², so based on the {001} surface, a supercell treatment was carried out to construct the silica crystal model. For the calcite surface, previous researchers found that the {104} surface is the most stable cleavage plane because of its most significant interlayer spacing and the lowest surface energy.³

2.3 Sealant-aggregate interface model

Through the interface construction tool in MS, the base bitumen, SBS-modified bitumen and epoxy resin sealant were combined with two kinds of aggregate mod-

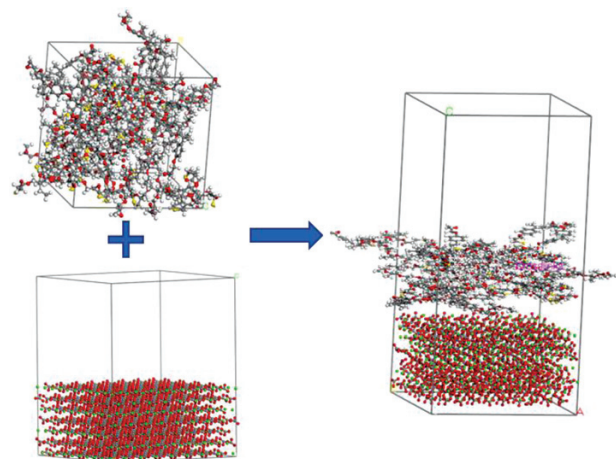


Figure 2: Epoxy binder-calcite interface model

els, respectively, to construct the sealant-aggregate interface model. In order to eliminate the influence of three-dimensional periodic boundary conditions on the Z-axis direction of the model, a 3-nm vacuum layer was added at the top of each bitumen-mineral interface model. When the model size was greater than (3.5×3.5) nm, the system energy converged and met the accuracy requirements, so an interface model with dimensions of (5×5) nm was finally constructed. Firstly, the energy minimization and geometric optimization of 5000 iterations were carried out on the constructed crack sealant-aggregate interface model. Then a 300-ps relaxation was carried out in the NVT ensemble to obtain a stable interface model of the system. After each model was balanced for 300 ps, a dynamic balance of 20 ps was performed on each interface model in the NPT ensemble to calculate the interface adhesion energy in the equilibrium state. In the molecular dynamic simulation of this section, a dynamic equilibrium is performed at 298 K, while the time step is 1 fs, and the truncation radius is 1.55 nm. The interface model of epoxy resin binder-calcite is shown in **Figure 2**.

2.4 Validation model

In molecular dynamics, density is often used to verify the reliability of a polymer molecular model in the MD simulation. This model was stable in the last nanosecond, and it fluctuated within a specific range. The model densities of base bitumen, SBS-modified bitumen and epoxy resin binder were $(1.004, 1.106$ and $1.032)$ g/cm³, respectively. The standard deviation of the density fluctuation was $0.006\text{--}0.035$ g/cm³, which is very small. Therefore, it was determined that all the models reached the equilibrium state in the last nanosecond, and the next analysis could be carried out.²⁴ The test densities of the three sealants were $(1.018, 1.024$ and $1.101)$ g/cm³, respectively. The relative errors of the calculated density of the base bitumen, SBS-modified bitumen, and epoxy

resin binder model simulated in this research were all within 5 % at 298 K, verifying the rationality of the simulation process.

3 STUDY OF THE SEALANT BASED ON MOLECULAR DYNAMICS

3.1 Physical properties of the sealant

3.1.1 Glass-transition temperature

In the low-temperature evaluation method for polymer materials, the glass-transition temperature T_g is commonly used to characterize the low-temperature properties of materials. Amorphous polymer materials undergo different states between low and high temperature: glassy state, glassy-rubber state and rubber state. When the sealant temperature is lower than its glass-transition temperature, the sealant in the glassy state is prone to interface cracking under temperature and traffic load stress, resulting in adhesive failure of the sealant. In this section, the glass-transition temperature of the three kinds of sealants was simulated with molecular dynamics to evaluate the low-temperature resistance of sealants. The simulation results are shown in **Figure 3**.

It can be seen from **Figure 3** that the glass-transition temperature of the base bitumen is 298 K, which is close to the simulation results provided by Liu²⁵ and Xu,²⁶ verifying the rationality of the model. In general, the simulated T_g is high, which is due to the significant influence of the simulation system conditions on the system energy. Compared with the experimental method, the polymer will lead to higher T_g within a molecular dynamics simulation.²⁷ However, the simulation trend is consistent with the actual situation. The order of the T_g of the three sealants from low to high is epoxy resin binder, SBS-modified bitumen and base bitumen. The rationality of the model is verified again. Moreover, it also shows that the low-temperature performance of the epoxy resin binder and SBS-modified bitumen is much higher than that of base bitumen, so they can better resist the adhesion failure of the crack interface at low temperatures.

3.1.2 Modulus

Bulk modulus, shear modulus, and Young's modulus can reflect the physical parameters of polymer materials' tensile, compressive, shear, and elastic properties, which are very important for the mechanical properties of a crack sealant. Bulk modulus can be used to evaluate the resistance of materials to compression or tension. Young's modulus measures the stiffness of isotropic elastomers, and shear modulus characterizes the ability of materials to resist a shear strain. In order to study the performance of a sealant, modulus parameters must be studied. In the molecular dynamics simulation, the modulus of the base bitumen, SBS-modified bitumen and epoxy resin sealant was calculated using the mechanical properties in the Forcite module of the MS software after structural optimization and dynamic relax-

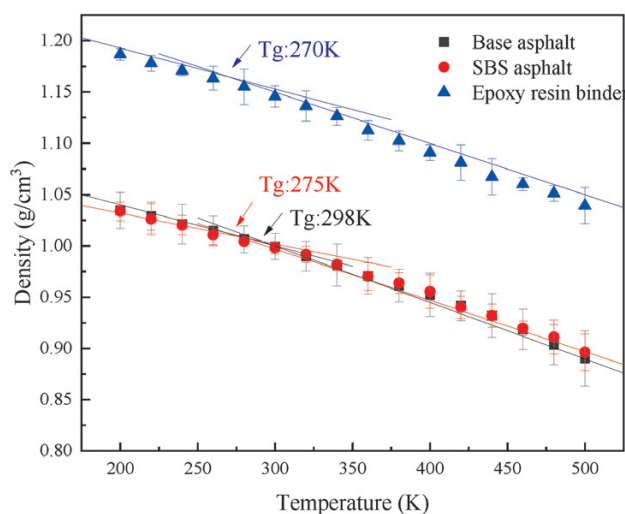


Figure 3: Glass-transition temperature of the sealants

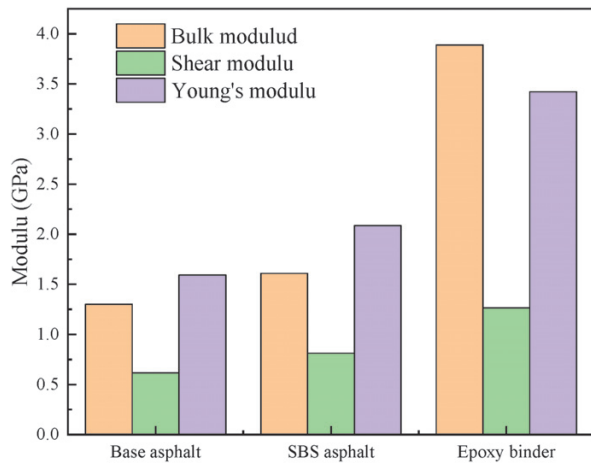


Figure 4: Simulation results for the modulus of the sealants

ation. In the Forcite module, mechanical properties were selected for the simulation. Mechanical parameters were solved with the constant strain method to calculate the encapsulant bulk modulus B and shear modulus S . The maximum values of bulk modulus and shear modulus were approximately calculated with the Voigt method. The minimum values were approximately calculated with the Reuss method. The modulus results of the two methods were modified with the VRH (Voigt-Reuss-Hill) approximation method proposed by Hill,²⁸ as shown in Equations (1) and (2).

Assuming that a sealant material is isotropic, Young's modulus of the sealant is calculated with Equation (3). Simulation results are shown in Figure 4.

$$B = B_{VRH} = \frac{B_V + B_R}{2} \tag{1}$$

$$S = S_{VRH} = \frac{S_V + S_R}{2} \tag{2}$$

$$E = \frac{9S}{3 + S/B} \tag{3}$$

It can be seen from Figure 4 that, regardless of the bulk modulus, shear modulus or Young's modulus, the descending order of the modulus values for the three kinds of crack sealants are the epoxy resin binder, SBS-modified bitumen and base bitumen. This shows that epoxy resin binder's resistance, stiffness and shear strain resistance to compression or tension are higher than those of bitumen grouting materials. Its bulk and Young's modulus are much higher than those of bitumen crack-grouting materials. This is because the cross-linking degree of the epoxy resin binder modified by the curing agent and diluent is 48 %, thus avoiding the problem of an insufficient toughness caused by complete curing, and having a unique three-dimensional network crosslinking structure. As a sealant, it has excellent mechanical properties and excellent flexibility. The addition of SBS also improves base bitumen's flexibility, stiffness, and crack resistance, indicating that SBS-modified bitumen has better physical properties.

3.2 Study of the sealant-aggregate interface

The biggest reason for the failure of the sealant lies in the failure of interface bonding, so it is necessary to study the adhesion of the sealant-aggregate interface. Many macroscopic tests are designed to evaluate the adhesion between a sealant and a crack wall, which plays an essential role in forming a solid bond. However, these tests cannot correlate adhesion with the microscopic composition of the sealant, while the MD simulation can assess adhesion on a microscopic scale. In molecular dynamics, adhesion work is used to evaluate interface adhesion. The work of adhesion is defined as the energy required to separate the interface into two free surfaces in a vacuum. In this definition, the greater the work of adhesion, the stronger are the bonding strength and stability of the interface. The calculated adhesion work of the bitumen-aggregate interface is shown in Equation (4):

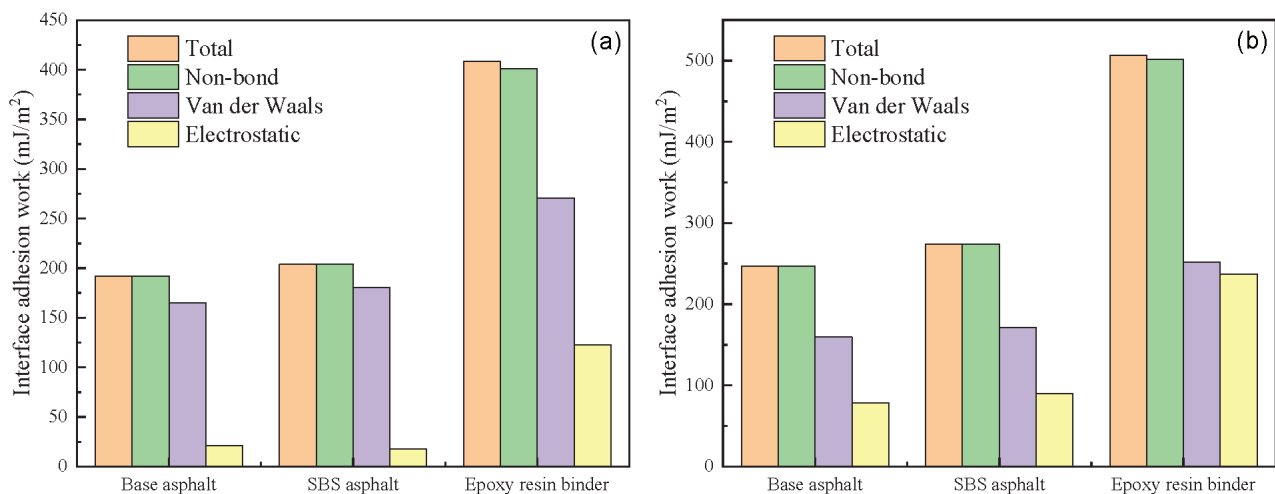


Figure 5: Adhesion work of the sealant-aggregate interface: a) silica, b) calcite

$$W_{as-agg} = \frac{E_{asphalt} + E_{aggregate} - E_{total}}{A} \quad (4)$$

where W_{as-agg} is the adhesion energy between the crack sealant and the aggregate interface (mJ/m^2); E_{total} is the total potential energy of the interface model after NVT equilibrium (mJ/m^2); $E_{asphalt}$ and $E_{aggregate}$ are the potential energy (mJ/m^2) of a single-crack sealant model and aggregate-surface model, respectively. A is the contact area (m^2) between the sealant and the mineral interface. The interaction energy of the three sealants and two aggregates was calculated using the Perl script, and then the adhesion work was calculated with Formula (4). The results are shown in **Figure 5**.

From **Figure 5**, it can be seen that the adhesion work of the sealant-aggregate interface is mainly generated by the non-bonded energy. The interaction between the three sealants and the aggregate is identified as mainly physical adsorption behavior. Different acid-base properties of the aggregate significantly affect the bonding performance of the sealant and aggregate. For the α -quartz-bitumen sealant model, the adhesion interaction is mainly determined by the van der Waals energy, and the electrostatic interaction has little effect. For the calcite-bitumen sealant model, the van der Waals interaction and electrostatic interaction are significant, but the overall impact is still greater than the van der Waals interaction. For the epoxy resin binder-aggregate model, whether an acidic aggregate or an alkaline one, the van der Waals and electrostatic interactions have a significant influence. The electrostatic interaction energy on the α -quartz interface is about half of the van der Waals interaction energy. The impacts of the van der Waals and electrostatic interaction energy on the calcite interface are similar. In general, the adhesion work of the three kinds of sealant-aggregate interface is greater for calcite than α -quartz, and the epoxy resin binder-aggregate interface adhesion work is the highest, indicating that the epoxy resin binder as a sealant exhibits excellent adhesion.

4 SURFACE ENERGY OF THE SEALANTS

In China, the aggregate used for the pavement is primarily alkaline rock. Therefore, based on the surface energy theory, this research studies the crack sealant-crack wall interface adhesion (the aggregate is limestone).

4.1 Surface energy theory

The surface energy theory can be used to calculate quantitatively the adhesion between two-phase materials. For the calculation of the interfacial free energy of the sealant-crack wall interface, formamide, ethylene glycol and distilled water, liquids with known polar components and dispersion components, are used. By measuring the contact angles of these liquids, potting sealants and crack walls, the polar components and dispersion components

of the sealant-crack wall are fitted and calculated, and the interfacial surface energy is obtained. The surface energy calculation is made with Equation (5):

$$\gamma = \gamma^d + \gamma^p \quad (5)$$

where γ is the surface free energy, mJ/m^2 ; γ^d is the dispersive component of surface free energy, mJ/m^2 ; γ^p is the polar component of the surface free energy, mJ/m^2 . The calculation of the adhesion work of two different materials (solid and liquid) is shown in Equation (6):

$$W_{sl} = 2\sqrt{\gamma_s^p \gamma_l^p} + 2\sqrt{\gamma_s^d \gamma_l^d} \quad (6)$$

where W_{sl} is the work of the solid-liquid interface adhesion; γ_s is the solid surface free energy; γ_l is the liquid surface free energy.

4.2 Surface energy calculation

The left and right contact angles of the three liquids (formamide, ethylene glycol, pure water) with known surface energy parameters and 90# base bitumen, SBS-modified bitumen, epoxy resin binder and limestone were measured with a contact angle meter. The average left and right contact angles of the three liquids with the above four materials were calculated. The polarity and dispersion components of different materials were calculated using the surface energy theory by fitting the average contact angle. The surface energy of different materials was calculated with Formula (5). The results are shown in **Table 4**.

Table 4: Surface energy of different materials and their dispersion and polarity components

Materials	Energy		
	Surface energy (mJ/m^2)	Polar component (mJ/m^2)	Dispersion component (mJ/m^2)
90# base bitumen	20.18	1.21	18.97
SBS-modified bitumen	22.50	2.69	19.81
Epoxy resin binder	33.41	28.43	4.98
SBS-bitumen mortar	22.01	2.34	19.67
Limestone	69.57	65.22	4.35

Table 4 and Equation (6) show that the adhesion work of 90# base bitumen, SBS-modified bitumen and epoxy resin binder with SBS-modified bitumen mortar and limestone aggregate was calculated, respectively. The calculation results are shown in **Figure 6**.

It can be seen from **Figure 6** that the adhesion-work order of the three crack sealants for the SBS-modified bitumen mortar at the crack wall is SBS-modified bitumen, base bitumen and the epoxy resin binder. However, the overall adhesion difference is not significant. This is because the compatibility between SBS-modified bitumen and SBS-modified bitumen mortar is higher than for the epoxy resin binder, and the adhesion work is more sig-

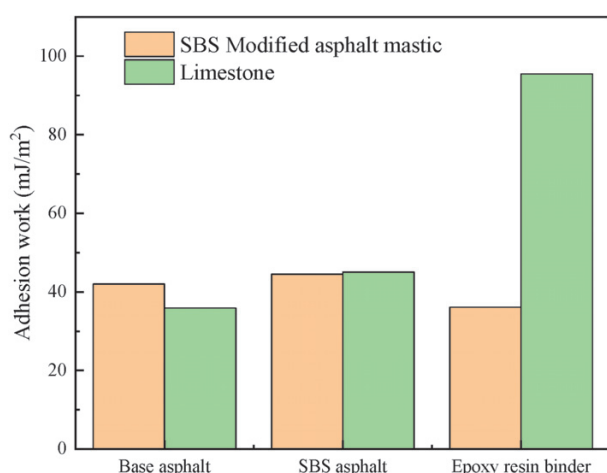


Figure 6: Adhesion work of different sealants with SBS-modified bitumen mortar and limestone aggregate

nificant. The adhesion-work order for limestone is the epoxy resin binder, SBS-modified bitumen and base bitumen. The adhesion work of the epoxy resin binder and limestone is more than twice that for SBS-modified bitumen, which is higher than that for the bitumen crack sealant.

In the AC-13 gradation, the aggregate accounts for more than 70 % of the bitumen mixture interface. According to the aggregate accounting for 70 % of the crack wall area, the adhesion work of 90# base bitumen, SBS-modified bitumen and epoxy resin binder for the asphalt pavement crack wall is (37.76, 44.86 and 77.63) mJ/m², respectively. The adhesion-work order of the three sealants and the crack wall is the epoxy resin binder, SBS-modified bitumen and 90# base bitumen. These results show that the epoxy resin binder exhibits excellent adhesion to crack walls as a crack sealant.

5 CONCLUSIONS

This paper used the molecular dynamics simulation method to study the physical properties of base bitumen, SBS-modified bitumen, epoxy resin sealant, and the adhesion properties of the sealant-aggregate interface. The adhesion of the sealant-crack wall was studied using a contact angle test based on the surface energy theory. The results are as follows:

1) The order of the T_g of the three crack sealants from low to high is epoxy resin binder, SBS-modified bitumen, and base bitumen. The low-temperature performance of epoxy resin binder and SBS-modified bitumen is excellent, so these can better resist the adhesion failure at low temperatures. The order of the modulus values of the three sealants from large to small is epoxy resin binder, SBS-modified bitumen and base bitumen. The compressive or tensile strength, stiffness and shear strain capacity of the epoxy sealant are higher than those of the bitumen sealant.

2) The adhesion work of the crack sealant-aggregate interface is generated by non-bonded energy. The adhesion work of the three kinds of crack sealant-aggregate interface shows that calcite is better than α -quartz, and the adhesion work of the epoxy resin binder-aggregate interface is the highest. For the α -quartz-bitumen sealant model, the adhesion interaction is mainly determined by the van der Waals energy, and the electrostatic interaction has little effect. For the calcite-bitumen crack sealant model, both the van der Waals interaction and electrostatic interaction are essential, but in general, the van der Waals interaction still has a more significant impact. For the epoxy resin binder-aggregate model, whether acidic aggregate or alkaline aggregate, the van der Waals and electrostatic interaction have a more significant impact.

3) The order of adhesion work of the three crack sealants at the crack wall is SBS-modified bitumen, base bitumen and epoxy resin binder. However, the overall adhesion difference is not significant. The order of adhesion work with limestone is epoxy resin binder, SBS-modified bitumen and base bitumen. The adhesion work of the epoxy resin binder with limestone is much higher than that of the bitumen crack sealant. The adhesion work of 90# base bitumen, SBS-modified bitumen and epoxy resin binder for a crack wall of an asphalt pavement is (37.76, 44.86 and 77.63) mJ/m², respectively, indicating that the epoxy resin binder exhibits excellent adhesion as a crack sealant for a crack wall of a bitumen mixture.

6 REFERENCES

- S. Liu, L. Mo, K. Wang, Y. Xie, M. F. Woldekidan, Preparation, microstructure and rheological properties of asphalt sealants for bridge expansion joints, *Construction and Building Materials*, 105 (2016), 1–13, doi:10.1016/j.conbuildmat.2015.12.017
- H. Zhang, Y. Bai, F. Cheng, Rheological and self-healing properties of asphalt binder containing microcapsules, *Construction and Building Materials*, 187 (2018), 138–148, doi:10.1016/j.conbuildmat.2018.07.172
- F. Li, S. Zhou, W. Cai, Y. Du, L. Li, Laboratory evaluation of short and long term performance of hot-poured sealants, *Construction and Building Materials*, 148 (2017), 30–37, doi:10.1016/j.conbuildmat.2017.05.014
- C. Plati, Sustainability factors in pavement materials, design, and preservation strategies: A literature review, *Construction and Building Materials*, 211 (2019), 539–555, doi:10.1016/j.conbuildmat.2019.03.242
- R. Gnatenko, K. Tsyrukunova, V. Zhdanuyuk, Technological Sides of Crack Sealing in Asphalt Pavements, *Transportation Research Procedia*, 14 (2016), 804–810, doi:10.1016/j.trpro.2016.05.028
- L. G. Diaz, Creep performance evaluation of Cold Mix Asphalt patching mixes, *International Journal of Pavement Research and Technology*, 9 (2016) 2, 149–158, doi:10.1016/j.ijprt.2016.04.002
- Y. Yildirim, Field performance comparison of asphalt crack-filling materials: hot pour versus cold pour, *Canadian Journal of Civil Engineering*, 34 (2007) 4, 505–512, doi:10.1139/106-143
- L. Cong, F. Yang, G. Guo, M. Ren, J. Shi, L. Tan, The use of polyurethane for asphalt pavement engineering applications: A state-of-the-art review, *Construction and Building Materials*, 225 (2019), 1012–1025, doi:10.1016/j.conbuildmat.2019.07.213

- ⁹ F. Li, Y. Du, L. Li, Viscoelastic Model and Stress Relaxation Evaluation of Pavement Crack Sealants at Low Temperature, *Journal of Materials in Civil Engineering*, 29 (2017) 9, doi:10.1061/(asce)mt.1943-5533.0001982
- ¹⁰ M. Sawalha, H. Ozer, I. L. Al-Qadi, H. Xue, Development of a Modified Adhesion Test for Hot-Poured Asphalt Crack Sealants, *Transportation Research Record: Journal of the Transportation Research Board*, 2612 (2017) 1, 85–95, doi:10.3141/2612-10
- ¹¹ E. G. Roozbahany, M. N. Partl, P. J. Witkiewicz, Fracture testing for the evaluation of asphalt pavement joints, *Road Materials and Pavement Design*, 14 (2013) 4, 764–791, doi:10.1080/14680629.2013.812979
- ¹² C. Peiliang, Y. Jianying, C. Shuanfa, Effects of epoxy resin contents on the rheological properties of epoxy-asphalt blends, *Journal of Applied Polymer Science*, 118 (2010) 6, 3678–3684, doi:10.1002/app.32440
- ¹³ Q. Xiang, F. Xiao, Applications of epoxy materials in pavement engineering, *Construction and Building Materials*, 235 (2020), doi:10.1016/j.conbuildmat.2019.117529
- ¹⁴ M. Liu, S. Han, J. Pan, W. Ren, Study on cohesion performance of waterborne epoxy resin emulsified asphalt as interlayer materials, *Construction and Building Materials*, 177 (2018), 72–82, doi:10.1016/j.conbuildmat.2018.05.043
- ¹⁵ A. Bhasin, R. Bommavaram, M. L. Greenfield, D. N. Little, Use of Molecular Dynamics to Investigate Self-Healing Mechanisms in Asphalt Binders, *Journal of Materials in Civil Engineering*, 23 (2011) 4, 485–492, doi:10.1061/(asce)mt.1943-5533.0000200
- ¹⁶ L. Zhang, M. L. Greenfield, Relaxation time, diffusion, and viscosity analysis of model asphalt systems using molecular simulation, *J. Chem. Phys.*, 127 (2007) 19, 194502, doi:10.1063/1.2799189
- ¹⁷ L. He, G. Li, S. Lv, J. Gao, K. J. Kowalski, J. Valentin, A. Alexiadis, Self-healing behavior of asphalt system based on molecular dynamics simulation, *Construction and Building Materials*, 254 (2020), doi:10.1016/j.conbuildmat.2020.119225
- ¹⁸ W. Sun, H. Wang, Self-healing of asphalt binder with cohesive failure: Insights from molecular dynamics simulation, *Construction and Building Materials*, 262 (2020), doi:10.1016/j.conbuildmat.2020.120538
- ¹⁹ D. D. Li, M. L. Greenfield, Chemical compositions of improved model asphalt systems for molecular simulations, *Fuel*, 115 (2014), 347–356, doi:10.1016/j.fuel.2013.07.012
- ²⁰ H-C. Dan, Z-M. Zou, Z. Zhang, J-W. Tan, Effects of aggregate type and SBS copolymer on the interfacial heat transport ability of asphalt mixture using molecular dynamics simulation, *Construction and Building Materials*, 250 (2020), doi:10.1016/j.conbuildmat.2020.118922
- ²¹ L. Luo, L. Chu, T. F. Fwa, Molecular dynamics analysis of moisture effect on asphalt-aggregate adhesion considering anisotropic mineral surfaces, *Applied Surface Science*, 527 (2020), doi:10.1016/j.apsusc.2020.146830
- ²² M. Kawasaki, K. Onuma, I. Sunagawa, Morphological instabilities during growth of a rough interface: AFM observations of cobbles on the (0001) face of synthetic quartz crystals, *Journal of Crystal Growth*, 258 (2003) 1–2, 188–196, doi:10.1016/s0022-0248(03)01509-4
- ²³ S. L. Stipp, M. F. Hochella, Structure and bonding environments at the calcite surface as observed with X-ray photoelectron spectroscopy (XPS) and low energy electron diffraction (LEED), *Geochimica et Cosmochimica Acta*, 55 (1991) 6, 1723–1736, doi:10.1016/0016-7037(91)90142-R
- ²⁴ L. Luo, L. Chu, T. F. Fwa, Molecular dynamics analysis of oxidative aging effects on thermodynamic and interfacial bonding properties of asphalt mixtures, *Construction and Building Materials*, 269 (2021), doi:10.1016/j.conbuildmat.2020.121299
- ²⁵ J. Liu, B. Yu, Q. Hong, Molecular dynamics simulation of distribution and adhesion of asphalt components on steel slag, *Construction and Building Materials*, 255 (2020), doi:10.1016/j.conbuildmat.2020.119332
- ²⁶ G. Xu, H. Wang, Molecular dynamics study of interfacial mechanical behavior between asphalt binder and mineral aggregate, *Construction and Building Materials*, 121 (2016), 246–254, doi:10.1016/j.conbuildmat.2016.05.167
- ²⁷ A. Soldera, N. Metatla, Glass transition of polymers: atomistic simulation versus experiments, *Phys. Rev. E. Stat. Nonlin. Soft. Matter. Phys.*, 74 (2006) 6, 061803, doi:10.1103/PhysRevE.74.061803
- ²⁸ R. Hill, The elastic behaviour of a crystalline aggregate, *Proceedings of the Physical Society. Section A*, 65 (1952) 5, 349